




Research article

DOI: <https://doi.org/10.18721/JCSTCS.17310>

UDC 303.732



## DEVELOPMENT OF AN OCT DATA CLASSIFICATION MODEL FOR DETERMINING THE PRESENCE AND TYPE OF OPHTHALMIC DISEASES

*L.E. Aksenova<sup>1</sup>  , K.D. Aksenov<sup>1</sup> ,  
A.V. Prysyzhnyuk<sup>1</sup>, V.V. Myasnikova<sup>2,1</sup>, A.V. Krasov<sup>3</sup>*

<sup>1</sup> LLC “Predict space”, Novorossiysk, Russian Federation;

<sup>2</sup> Maykop State Technological University, Maykop, Russian Federation;

<sup>3</sup> Bonch-Bruевич St. Petersburg State University of Telecommunications,  
St. Petersburg, Russian Federation

 axenovalubov@gmail.com

**Abstract.** Optical Coherence Tomography (OCT) is an important tool in the diagnosis of common ophthalmological diseases, such as age-related macular degeneration and diabetic retinopathy. However, the processes of analyzing and interpreting OCT data are highly complex due to the need to process a large amount of data and the time spent on research, as well as the ophthalmologist's failure to recognize minor or early signs of the disease or rare pathologies. This paper proposes a comprehensive approach to the development of an OCT image analysis system based on deep neural networks. In particular, the performance of models based on four neural network architectures – ResNet50, VGG16, InceptionV4, and ResNet101 – was evaluated. The results show that the model based on the ResNet50 architecture achieves the highest proportion of correctly classified images. Furthermore, the integration of the developed model into a chatbot significantly reduces the time needed to interpret OCT images, which can contribute to increased availability of preliminary diagnostics and improved quality of medical services.

**Keywords:** artificial intelligence, ophthalmology, machine learning models, neural network architectures, convolutional neural networks, optical coherence tomography, chatbot

**Acknowledgements:** The research was financially supported by a grant from the Foundation for Assistance to Small Innovative Enterprises in Science and Technology (FASIE) based on the results of the “Start-23-1 (stage II)” competition, the project “Intelligent system for OCT data analysis EyeTech” (agreement No. 5064GS1/89527 dated October 30, 2023).

**Citation:** Aksenova L.E., Aksenov A.K., Prysyzhnyuk A.V., et al. Development of an OCT data classification model for determining the presence and type of ophthalmic diseases. *Computing, Telecommunications and Control*, 2024, Vol. 17, No. 3, Pp. 103–113. DOI: 10.18721/JCSTCS.17310



Научная статья

DOI: <https://doi.org/10.18721/JCSTCS.17310>

УДК 303.732



## РАЗРАБОТКА МОДЕЛИ КЛАССИФИКАЦИИ ДАННЫХ ОКТ ДЛЯ ОПРЕДЕЛЕНИЯ НАЛИЧИЯ И ТИПА ОФТАЛЬМОЛОГИЧЕСКИХ ЗАБОЛЕВАНИЙ

Л.Е. Аксенова<sup>1</sup> , К.Д. Аксенов<sup>1</sup> ,  
А.В. Присяжнюк<sup>1</sup>, В.В. Мясникова<sup>2,1</sup>, А.В. Красов<sup>3</sup>

<sup>1</sup> ООО «Пространство интеллектуальных решений»,  
Новороссийск, Российская Федерация;

<sup>2</sup> Майкопский государственный технологический университет,  
Майкоп, Российская Федерация;

<sup>3</sup> Санкт-Петербургский государственный университет телекоммуникаций  
им. проф. М.А. Бонч-Бруевича, Санкт-Петербург, Российская Федерация

✉ axenovalubov@gmail.com

**Аннотация.** Оптическая когерентная томография (ОКТ) является важным инструментом в диагностике распространенных офтальмологических заболеваний, таких как возрастная макулярная дегенерация и диабетическая ретинопатия. Тем не менее, процессы анализа и интерпретации данных ОКТ представляют высокую сложность как в виду необходимости анализа большого количества данных и затраченного на исследования времени, так и пропуска незначительных и ранних признаков заболевания или редких патологий врачом офтальмологом. В настоящей работе предложен комплексный подход к разработке системы анализа изображений ОКТ на основе глубоких нейронных сетей. В частности, была проведена оценка производительности моделей на основе четырех архитектур нейронных сетей – ResNet50, VGG16, InceptionV4 и ResNet101. Результаты показывают, что модель на основе архитектуры ResNet50 позволяет достичь наибольшей доли правильно классифицированных изображений. Кроме того, внедрение разработанной модели в чат-бот позволяет существенно сократить время интерпретации ОКТ изображений, что может способствовать увеличению доступности предварительной диагностики и улучшению качества оказания медицинских услуг.

**Ключевые слова:** искусственный интеллект, офтальмология, модели машинного обучения, архитектуры нейронных сетей, сверточные нейронные сети, оптическая когерентная томография, чат-бот

**Финансирование:** Исследование выполнено при поддержке гранта Фонда содействия инновациям по результатам конкурса «Старт-23-1 (очередь II)», проект «Интеллектуальная система анализа данных ОКТ “EyeTech”» (договор № 5064ГС1/89527 от 30.10.2023).

**Для цитирования:** Aksenova L.E., Aksenov A.K., Prisyazhnyuk A.V., et al. Development of an OCT data classification model for determining the presence and type of ophthalmic diseases // Computing, Telecommunications and Control. 2024. Т. 17, № 3. С. 103–113. DOI: 10.18721/JCSTCS.17310

### Introduction

According to the World Health Organization (WHO), some of the most common ophthalmic diseases are age-related macular degeneration (AMD) and diabetic retinopathy (DR). At the same time, vision-related diseases often lack obvious symptoms in the early stages and are easily overlooked by patients, leading to irreversible vision impairment by the time they visit the clinic [1]. Optical Coherence Tomography (OCT) is widely used in ophthalmology and is considered the gold standard for early diagnosis of many diseases, identification of prognostic biomarkers, monitoring disease progression, and evaluating patient

response to treatment [2]. OCT is a non-invasive imaging method that allows for high-resolution imaging of eye structures, with a resolution of up to 1–5 microns [3]. However, the analysis and interpretation of OCT data are complex due to the need to analyze large volumes of data and the time-consuming nature of the research, as well as the possibility of missing minor and early signs of disease or rare pathologies by an ophthalmologist [4].

In recent years, with the development of artificial intelligence (AI) technologies and machine learning, there has been growing interest in applying these methods to automate the process of OCT image analysis. A distinctive feature of OCT data, as well as other medical data, is the subtle structural changes that can indicate the presence of disease. For example, disease identification often requires not only detecting pathology, but also determining its location and volume [5]. Traditional image processing methods cannot effectively identify such small anomalies, which necessitates the use of more sophisticated deep learning (DL) models capable of accounting for spatial and contextual dependencies within OCT images [6]. According to the research, systems based on such AI technologies as deep neural networks (DNN) can significantly improve the accuracy and speed of diagnosing ophthalmic diseases [7, 8].

A key factor in the development of AI technologies in the field of medicine is the availability of high-quality datasets [9]. To date, numerous results have been obtained using open datasets for creating models for analyzing OCT images [10–12]. Moreover, a key task in the development of AI systems for OCT image analysis is choosing a neural network architecture that will efficiently perform classification tasks. The most common types of networks are Convolutional Neural Networks (CNNs), whose main distinguishing feature is their ability to account for spatial hierarchical dependencies in data, allowing them to effectively identify complex patterns and structures in the images [8, 9, 13]. An important aspect of choosing a neural network architecture is also the balance between model complexity and the required computational resources. One promising direction in this area is the use of transfer learning, which allows pre-trained models on large datasets to be adapted to a specific OCT image classification task. The works [14, 15] show that transfer learning can significantly improve classification results, especially in the conditions of limited training data.

The novelty of this study is the creation of a comprehensive OCT image analysis system that integrates various modules, including segmentation, classification, and quantitative assessment of biomarkers. In previous stages of the research, we developed and tested a segmentation model using clinical data for determining the type and quantitative parameters of biomarkers on OCT images [16]. The aim of this study was to compare the effectiveness of different neural network architectures for the task of OCT image classification to develop a disease classification module. The practical significance of this work is the integration of the neural network based model with the best accuracy into a chatbot to support doctors and patients by providing automatic interpretations and recommendations.

### Materials and Methods

In this study, we used the publicly available OCTDL dataset, which consists of 2064 images from 821 patients [10]. The images are B-scans in .jpg format obtained using the Optovue Avanti RTVue XR optical coherence tomography scanner with a raster scan protocol. The images were grouped into the following categories:

- Age-related Macular Degeneration (AMD),
- Diabetic Macular Edema (DME),
- Epiretinal Membrane (ERM),
- Normal (NO),
- Retinal Arterial Occlusion (RAO),
- Retinal Venous Occlusion (RVO),
- Vitreomacular Interface Disorder (VID) (Fig. 1).

Table 1 provides a description of the dataset. The entire dataset was divided into training, validation, and test sets in a 65/15/20 ratio to achieve an optimal balance between the amount of data for training

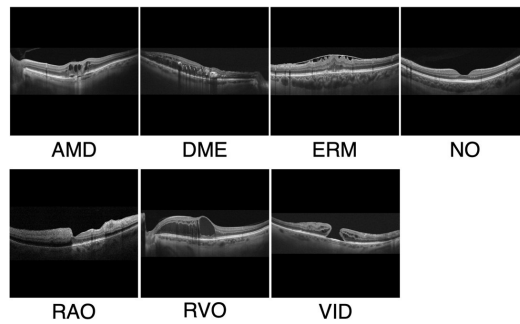


Fig. 1. Examples of the images from the publicly available OCTDL dataset

and evaluation on the independent images (Fig. 2). The distribution of images across the subsets also considered the proportion of each class in the overall dataset to minimize the impact of class imbalance.

Table 1

**Distribution of image classes in the training, validation and test sets**

Class	Training Set	Validation Set	Test Set	Total Images
AMD	801	192	238	1231
DME	96	21	30	147
ERM	100	20	35	155
NO	216	36	80	332
RAO	12	1	9	22
RVO	66	13	22	101
VID	49	12	15	76

For the classification of OCT images, we used four types of DNNs: ResNet50, ResNet101, InceptionV4, and VGG16. These architectures have shown efficiency in the image recognition for tasks such as skin cancer diagnosis [17], early-stage Alzheimer’s disease detection [18], and retinal vessel detection in fundus images [19], as well as in quality assessment and classification of OCT images [20, 21].

The neural network architectures ResNet50, ResNet101, InceptionV4, and VGG16 are deep CNNs with varying numbers of layers, which were pretrained on large image datasets, such as ImageNet [22]. ResNet50 consists of 50 layers and employs “residual blocks.” ResNet101 has a similar structure, but comprises 101 layers. InceptionV4 is a DNN with 22 layers that includes “Inception modules” designed to reduce parameters, speed up computations, and prevent overfitting [23]. The VGG16 architecture includes 13 convolutional layers, 5 pooling layers, and 3 fully connected layers, and it has a simple and deep structure [9]. Prior to training the models, we performed data preprocessing and augmentation. The preprocessing involved resizing images to 224x224 pixels, and augmentation techniques included random cropping, horizontal and vertical flipping, rotation, shifting, and Gaussian blurring. The performance of the models was evaluated using the following metrics: Accuracy (1), Precision (2), Recall (3), F1 Score (4), and AUC-ROC.

Accuracy (the proportion of correctly classified objects) measures the proportion of correct predictions among all predictions. This is a basic metric for assessing the overall effectiveness of a model.

$$\text{Accuracy} = \frac{TP + TN}{TP + TN + FP + FN}, \quad (1)$$



Fig. 2. Visualization of the distribution of images across datasets

where  $TP$  are True Positives,  $TN$  are True Negatives,  $FP$  are False Positives, and  $FN$  are False Negatives.

Precision (proportion of true positive results) measures the proportion of true positive results among all results classified as positive:

$$\text{Precision} = \frac{TP}{TP + FP}. \quad (2)$$

Recall measures the proportion of true positive results among all actual positive cases:

$$\text{Recall} = \frac{TP}{TP + FN}. \quad (3)$$

F1 Score is the harmonic mean of precision and recall, making it useful in tasks, where the balance between the precision and the recall is important:

$$\text{F1 Score} = 2 \times \frac{\text{Precision} \times \text{Recall}}{\text{Precision} + \text{Recall}}. \quad (4)$$

AUC-ROC (Area under the Receiver Operating Characteristic Curve) is a measure of the model's ability to distinguish between classes. The ROC curve is a plot that shows the model's performance at all classification thresholds. AUC-ROC is calculated as the area under the ROC curve, which is constructed based on different values of sensitivity (recall) and specificity ( $1 - \text{False Positive Rate}$ ). These metrics were calculated for each class using the "one vs rest" method. To evaluate the metrics for the entire dataset, the average value of the obtained metrics was calculated. As performance characteristics of machine learning models, training time, prediction time, and the number of parameters were measured.

For training the models, we used the early stopping algorithm. Early stopping was triggered, when the Accuracy metric, measured on the validation dataset, reached its maximum value.

Training and evaluation of the models were performed using the PyTorch DL framework (version 2.1.1) and cloud resources from Yandex Cloud (Yandex Cloud Documentation), which were provided as a part of the Yandex Cloud Boost program in a configuration with vCPUs on the Intel Broadwell platform and GPU NVIDIA® Tesla® V100.

To ensure user interaction with the model, an infrastructure was developed that included a chatbot<sup>1</sup> integrated with the DL model. For integrating the model into the chatbot, a server-side component was created in Python using the Django framework. To ensure flexibility and scalability, the system was containerized using Docker and deployed on Yandex Cloud resources.

### Results and Discussion

In this study, models incorporating neural network architectures, such as VGG16, InceptionV4, ResNet50, and ResNet101 were trained on the OCTDL open dataset. To evaluate the performance of the models, metrics, such as Accuracy, F1 Score, Precision, Recall, and AUC-ROC were calculated, along with efficiency characteristics. Table 2 presents the metric values measured on the test set across all the classes for four models.

Table 2

#### Quantitative performance indicators of machine learning models

	ResNet50	VGG16	InceptionV4	ResNet101
Accuracy	0.93	0.92	0.93	0.91
F1 Score	0.89	0.87	0.89	0.86
Precision	0.88	0.86	0.89	0.87
Recall	0.91	0.9	0.89	0.86
AUC-ROC	0.99	0.99	0.98	0.99
Number of Epochs	100	100	100	100
Training Time (seconds)	2913	3243	1890	1032
Prediction Time (seconds)	32	38	29	20
Number of Training Parameters (millions)	25.6	138	42.7	44.5

All four models demonstrated relatively high accuracy. The model with the ResNet50 architecture achieved the highest values for Accuracy (0.93), F1 Score (0.89), Recall (0.91), and AUC-ROC (0.99). InceptionV4 also achieved the same values for Accuracy and F1 Score. However, the Precision value (0.89) for this architecture was the highest among all, while Recall and AUC-ROC were 0.89 and 0.98, respectively.

Table 3 provides the performance values for the classification of individual ophthalmic disease classes. All models show satisfactory Accuracy values (above 0.8) for all classes. The Accuracy value for the RAO class is 1, which is associated with a lack of data in the test sample.

Fig. 3 allows for a visual comparison of accuracy values across four different neural network architectures — ResNet50, VGG16, InceptionV4, and ResNet101 — relative to metrics, such as Precision, Recall, and F1 Score. The graph shows that ResNet50 and InceptionV4 architectures demonstrate the most stable and highest metric values for almost all the classes of ophthalmic diseases. A noticeable decrease in accuracy is observed for the VGG16 model for the RVO class, which may be related to the insufficient volume of data for this class.

Fig. 4 shows the results of the confusion matrix calculation relative to the classes of ophthalmic diseases for four neural network architectures. The most undesirable outcome in the clinical practice of automated algorithms is classifying a normal image, when there is a pathology present. From the table, it can be concluded that the ResNet50 and InceptionV4 architectures only misclassified in the AMD class, which was the most represented class in the test dataset. The VGG16 and ResNet101 architectures misclassified both AMD and ERM classes.

<sup>1</sup> Telegram: Contact @eye\_tech\_bot. Available: [https://t.me/eye\\_tech\\_bot](https://t.me/eye_tech_bot) (accessed 11.10.2024)

Table 3

**Performance values for the classification of individual ophthalmic disease classes**

ResNet50				
Class	Precision	Recall	F1 Score	Total images
AMD	0.97	0.96	0.97	238
DME	0.82	0.90	0.86	30
ERM	0.86	0.91	0.89	35
NO	0.92	0.88	0.90	80
RAO	1.00	1.00	1.00	9
RVO	0.74	0.77	0.76	22
VID	0.82	0.93	0.87	15
VGG16				
AMD	0.99	0.95	0.97	238
DME	0.76	0.93	0.84	30
ERM	0.78	0.91	0.84	35
NO	0.95	0.90	0.92	80
RAO	1.00	1.00	1.00	9
RVO	0.82	0.64	0.72	22
VID	0.74	0.93	0.82	15
InceptionV4				
AMD	0.97	0.95	0.96	238
DME	0.79	0.90	0.84	30
ERM	0.87	0.94	0.90	35
NO	0.92	0.91	0.92	80
RAO	1.00	1.00	1.00	9
RVO	0.75	0.68	0.71	22
VID	0.93	0.87	0.90	15
ResNet101				
AMD	0.97	0.96	0.97	238
DME	0.81	0.87	0.84	30
ERM	0.75	0.94	0.84	35
NO	0.92	0.88	0.90	80
RAO	1.00	1.00	1.00	9
RVO	0.70	0.64	0.67	22
VID	0.92	0.73	0.81	15

Neural network architectures, such as ResNet50, ResNet101, InceptionV4, and VGG16, have also been used by other researchers for image classification tasks. In [11], the OCTDL dataset was employed to train VGG16 and ResNet50 models. The Accuracy, F1 Score, and Recall values for the ResNet50 architecture were lower than those obtained in the current study, by 0.8, 0.2, and 0.6, respectively [10]. In [13, 23], the high efficiency of ResNet and Inception101 models for medical image classification tasks was demonstrated. In [8], the ResNet model achieved an accuracy of 0.97 for OCT image classification, while in [5] an accuracy of 0.95 using an Inception-based model was achieved.



Fig. 3. The results of evaluating the accuracy of machine learning models for each class

The developed model was integrated into a chatbot. The response time for producing results is less than 1 sec, ensuring prompt feedback and enabling rapid analysis even with a high data flow. An example of the response received by a user through the chatbot is shown in Fig. 5. This study did not compare these results with the speed of data assessment by clinicians. Nevertheless, according to the literature, an AI system for radiological image analysis reduced the interpretation time from 11.2 to 2.7 days, highlighting the efficiency of automated systems in optimizing healthcare workflows and improving patient care standards [24].



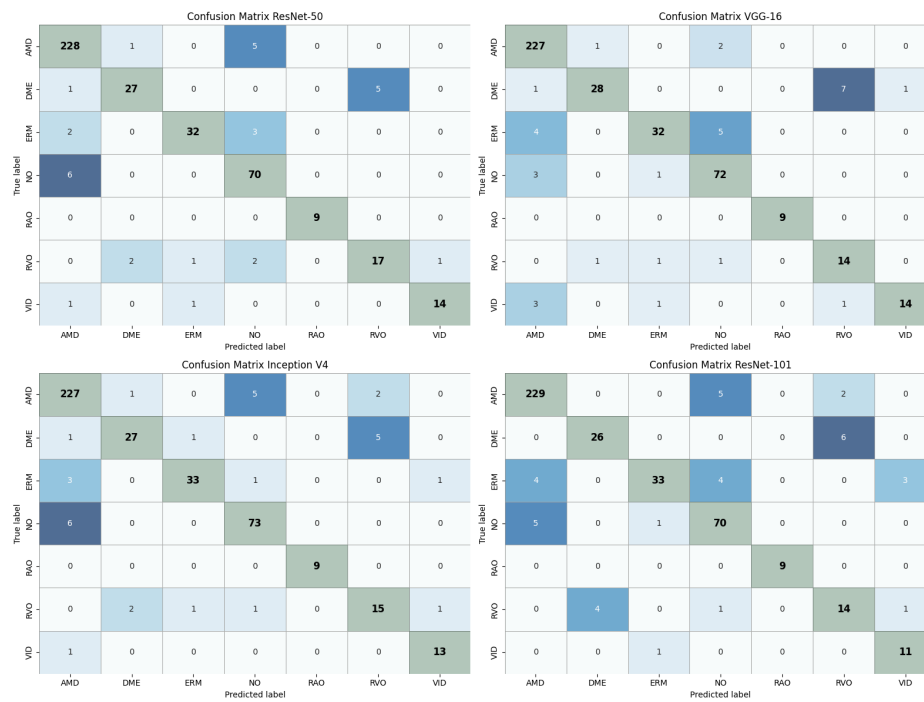


Fig. 4. Confusion matrix for four neural network architectures



Fig. 5. An example of OCT data analysis results using a chatbot integrated with a model based on the ResNet50 architecture. The results for image 2. Classification results:  
 1. Age-related macular degeneration – 98.13%; 2. Norm – 0.61%; 3. Vitreomacular traction – 0.39%

### Conclusion

In this study, we identified the model with the highest accuracy for evaluating seven classes of ophthalmological diseases. This model is integrated into the chatbot and provides the doctor with a preliminary result of the presence of a pathology in less than 1 second. Thus, the results of this study significantly simplify and accelerate the process of data analysis for ophthalmologists, as well as allow patients to receive an initial consultation anytime and anywhere.

## REFERENCES

1. **Steinmetz J.D., Bourne R.R.A., Briant P.S. et al.** GBD 2019 Blindness and Vision Impairment collaborators. Causes of blindness and vision impairment in 2020 and trends over 30 years, and prevalence of avoidable blindness in relation to VISION 2020: the Right to Sight: an analysis for the Global Burden of Disease Study. *The Lancet Global Health*, 2021, Vol. 9, No. 2, Pp. e144–e160. DOI: 10.1016/S2214-109X(20)30489-7
2. **Zeppieri M., Marsili S., Enaholo E.S., Shuaibu A.O., Uwagboe N., Salati C., Spadea L., Musa M.** Optical Coherence Tomography (OCT): A Brief Look at the Uses and Technological Evolution of Ophthalmology. *Medicina*, 2023, Vol. 59, No. 12, Article no. 2114. DOI: 10.3390/medicina59122114
3. **Zheng S., Bai Y., Xu Z., Liu P., Ni G.** Optical Coherence Tomography for Three-Dimensional Imaging in the Biomedical Field: A Review. *Frontiers in Physics*, 2021, Vol. 9, Article no. 744346. DOI: 10.3389/fphy.2021.744346
4. **Hussain A., Oestreicher J.** Clinical decision-making: heuristics and cognitive biases for the ophthalmologist. *Survey of Ophthalmology*, 2018, Vol. 63, No. 1, Pp. 119–124. DOI: 10.1016/j.survophthal.2017.08.007
5. **De Fauw J., Ledsam J.R., Romera-Paredes B. et al.** Clinically applicable deep learning for diagnosis and referral in retinal disease. *Nature Medicine*, 2018, Vol. 24, Pp. 1342–1350. DOI: 10.1038/s41591-018-0107-6
6. **Wang J., Hormel T.T., Gao L., Zang P., Guo Y., Wang X., Bailey S.T., Jia Y.** Automated diagnosis and segmentation of choroidal neovascularization in OCT angiography using deep learning. *Biomedical Optics Express*, 2020, Vol. 11, Pp. 927–944. DOI: 10.1364/BOE.379977
7. **Grassmann F., Mengelkamp J., Brandl C., Harsch S., Zimmermann M.E., Linkohr B., Peters A., Heid I.M., Palm C., Weber B.H.F.** A Deep Learning Algorithm for Prediction of Age-Related Eye Disease Study Severity Scale for Age-Related Macular Degeneration from Color Fundus Photography. *Ophthalmology*, 2018, Vol. 125, No. 9, Pp. 1410–1420. DOI: 10.1016/j.ophtha.2018.02.037
8. **Kermany D.S., Goldbaum M., Cai W. et al.** Identifying Medical Diagnoses and Treatable Diseases by Image-Based Deep Learning. *Cell*, 2018, Vol. 172, No. 5, Pp. 1122–1131. DOI: 10.1016/j.cell.2018.02.010
9. **Simonyan K., Zisserman A.** Very Deep Convolutional Networks for Large-Scale Image Recognition. 3<sup>rd</sup> International Conference on Learning Representations (ICLR 2015), 2015, Pp. 1–14.
10. **Kulyabin M., Zhdanov A., Nikiforova A. et al.** OCTDL: Optical Coherence Tomography Dataset for Image-Based Deep Learning Methods. *Scientific Data*, 2024, Vol. 11, Article no. 365. DOI: 10.1038/s41597-024-03182-7
11. **Gholami P., Roy P., Parthasarathy M.K., Lakshminarayanan V.** OCTID: Optical Coherence Tomography Image Database. *Computers and Electrical Engineering*, 2018, Vol. 81, Article no. 106532. DOI: 10.1016/j.compeleceng.2019.106532
12. **Kermany D., Zhang K., Goldbaum M.** Labeled Optical Coherence Tomography (OCT) and Chest X-Ray Images for Classification. *Mendeley Data*, 2018, V2. DOI: 10.17632/rsbjbr9sj.2
13. **He K., Zhang X., Ren S., Sun J.** Deep Residual Learning for Image Recognition. 2016 IEEE Conference on Computer Vision and Pattern Recognition (CVPR), 2016, Pp. 770–778. DOI: 10.1109/CVPR.2016.90
14. **Shin H.C., Roth H.R., Gao M., Lu L., Xu Z., Noguez I., Yao J., Mollura D., Summers R.M.** Deep Convolutional Neural Networks for Computer-Aided Detection: CNN Architectures, Dataset Characteristics and Transfer Learning. *IEEE Transactions on Medical Imaging*, 2016, Vol. 35, No. 5, Pp. 1285–1298. DOI: 10.1109/TMI.2016.2528162
15. **Tajbakhsh N., Shin J.Y., Gurudu S.R., Hurst R.T., Kendall C.B., Gotway M.B., Liang J.** Convolutional Neural Networks for Medical Image Analysis: Full Training or Fine Tuning? *IEEE Transactions on Medical Imaging*, 2016, Vol. 35, No. 5, Pp. 1299–1312. DOI: 10.1109/TMI.2016.2535302
16. **Aksenova L.E., Aksenov K.D., Kozina E.V., Myasnikova V.V.** Automated System for Analysis of OCT Retina Images Development and Testing. *Doklady Mathematics*, 2024, Vol. 108, Pp. 310–316. DOI: 10.1134/S1064562423701545

17. **Esteva A., Kuprel B., Novoa R. et al.** Dermatologist-level classification of skin cancer with deep neural networks. *Nature*, 2017, Vol. 542, Pp. 115–118. DOI: 10.1038/nature21056
18. Liu S., Liu S., Cai W., Pujol S., Kikinis R., Feng D. Early diagnosis of Alzheimer’s disease with deep learning. 2014 IEEE 11<sup>th</sup> International Symposium on Biomedical Imaging (ISBI), 2014, Pp. 1015–1018. DOI: 10.1109/ISBI.2014.6868045
19. **Maji D., Santara A., Ghosh S., Sheet D., Mitra P.** Deep neural network and random forest hybrid architecture for learning to detect retinal vessels in fundus images. 2015 37<sup>th</sup> Annual International Conference of the IEEE Engineering in Medicine and Biology Society (EMBC), 2015, Pp. 3029–3032. DOI: 10.1109/EMBC.2015.7319030
20. **Subramanian M., Shanmugavadivel K., Naren O.S., Premkumar K., Rankish K.** Classification of Retinal OCT Images Using Deep Learning. 2022 International Conference on Computer Communication and Informatics (ICCCI), 2022, Pp. 1–7. DOI: 10.1109/ICCCI54379.2022.9740985
21. **Inferrera L., Borsatti L., Miladinovic A., Marangoni D., Giglio R., Accardo A., Tognetto D.** OCT-based deep-learning models for the identification of retinal key signs. *Scientific Reports*, 2023, Vol. 13, Article no. 14628. DOI: 10.1038/S41598-023-41362-4
22. **Krizhevsky A., Sutskever I., Hinton G.E.** ImageNet Classification with Deep Convolutional Neural Networks. *Communications of the ACM*, 2017, Vol. 60, No. 6, Pp. 84–90. DOI: 10.1145/3065386
23. **Szegedy C. et al.** Going deeper with convolutions. 2015 IEEE Conference on Computer Vision and Pattern Recognition (CVPR), 2015, Pp. 1–9. DOI: 10.1109/CVPR.2015.7298594
24. **Annarumma M., Withey S.J., Bakewell R.J., Pesce E., Goh V., Montana G.** Automated Triaging of Adult Chest Radiographs with Deep Artificial Neural Networks. *Radiology*, 2019, Vol. 291, No. 1, Pp. 196–202. DOI: 10.1148/radiol.2018180921

#### INFORMATION ABOUT AUTHORS / СВЕДЕНИЯ ОБ АВТОРАХ

**Aksenova Lyubov E.**

**Аксенова Любовь Евгеньевна**

E-mail: axenovalubov@gmail.com

ORCID: <https://orcid.org/0000-0003-0885-1355>

**Aksenov Kirill D.**

**Аксенов Кирилл Дмитриевич**

E-mail: axenov.kir@gmail.com

ORCID: <https://orcid.org/0000-0001-5391-5229>

**Prsyazhnyuk Anton V.**

**Присяжнюк Антон Владимирович**

E-mail: kagehitori@gmail.com

**Myasnikova Viktoria V.**

**Мясникова Виктория Владимировна**

E-mail: vivlad7@mail.ru

**Krasov Andrei V.**

**Красов Андрей Владимирович**

E-mail: krasov@inbox.ru

*Submitted: 15.06.2024; Approved: 24.09.2024; Accepted: 04.10.2024.*

*Поступила: 15.06.2024; Одобрена: 24.09.2024; Принята: 04.10.2024.*